Detecting Short-wavelength Infrared Photons by Schottky-barrier based Single Photon Avalanche Diode in 180-nm CMOS Technology

Chun-Hsien Liu
Institute of Electronics
National Yang Ming Chiao Tung University
Hsinchu, Taiwan
terryliu225.ee07@nycu.edu.tw

Yu-Wei Lue
Institute of Electronics
National Yang Ming Chiao Tung University
Hsinchu, Taiwan

Sheng-Di Lin
Institute of Electronics
National Yang Ming Chiao Tung University
Hsinchu, Taiwan

***Abstract*—We propose a Schottky-barrier (SB) based single-photon avalanche diode (SPAD) in 180-nm CMOS technology. SB-based SPAD consisted of Schottky junction as active region can detect short-wavelength infrared photons by internal photoemission effect. The simulated strong electric field for triggering avalanche process ensures multiplication region locating at the active region. The preliminary measurement obtained the responsivity of ~60 mA/W in 1550 nm at 15 V, the dark count rate ranged 10 kHz – 2 MHz, and photon detection probability of ~0.35% at excess bias voltage of 1.0 V.**

Keywords—Single photon avalanche diode, Short wavelength infrared sensor

I. Introduction

CMOS single-photon avalanche diode (SPAD) has excellent photo-sensitivity and timing response and serves as a receiver in light detection and ranging (LiDAR) [1]. For LiDAR application, short-wavelength infrared (SWIR) sensors have been attractive because of its safety level of maximum exposure intensity is much higher than that in near infrared regime and more laser power could give a longer detectable distance [2]. Due to silicon bandgap of 1.12 eV, silicon-based SPAD could not detect SWIR photons. To realize SWIR detection, researchers have turned to other materials such as Ge-on-Si SPAD, III-V SPAD or superconducting nanowire detector (SNSPD) [3-5]. In this work, we propose a Schottky barrier (SB) based SPAD fabricated in 180-nm CMOS technology with the detection wavelength range up to 1550 nm. The previous work [6] demonstrated SWIR photocurrent measurement using silicon-based Schottky diodes even the photon energy is lower than silicon bandgap due to the photon-absorption induced internal photoemission (IPE) effect [7]. Figure 1 illustrates the various SWIR photon detection mechanisms in a Schottky diode.

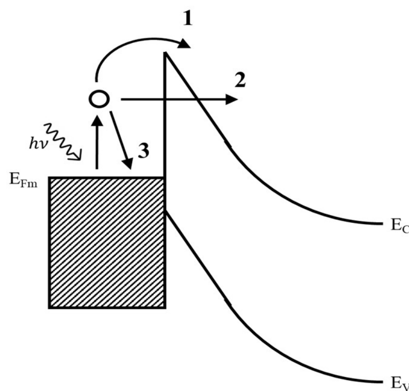

Figure 1. Photon-absorption induced internal photoemission (IPE) effect, and three possible paths, (1) hot electrons emission, (2) cold-field emission, and (3) recombination.

Path 1 is the best because the photo-generated energetic electrons have the highest efficiency to cross barrier. Path 2 is the cold-field emission and allows photon with energy lower than Schottky barrier height to be collected via quantum tunneling. The worst one is path 3 because the electrons could not cross the barrier to contribute any photocurrent. Therefore, the detectable longest wavelength is dominated by the Schottky barrier height. In this work, we propose a SWIR detector with Schottky-barrier based SPAD and show the simulate structure and breakdown simulation with technology computer aided design (TCAD) and descript our measurement environment in the section two. The device experiment results of electric and optical characteristics are shown and discussed in section three.

II. Device and Measurement

Figure 2 shows the designed structure of our Schottky-SPAD in 180-nm CMOS process without any customization. The device has a square-shape active area with a size of 10 μm. To detect SWIR, a Schottky barrier for photo-generated hot electrons to overcome from the metal into bulk silicon by IPE. The injected electrons are then accelerated by the underneath strong electric field and amplified as a voltage signal. The Schottky junction was formed between cobalt silicide (CoSi2) and high-voltage n-type well (HVNW) layer.

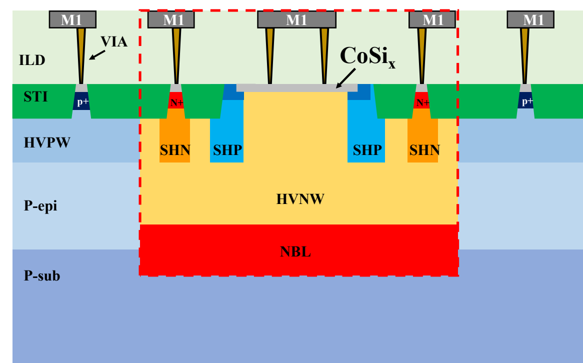

Figure 2. Schematic of the Schottky SPAD in cross-section view.

XXX-X-XXXX-XXXX-X/XX/$XX.00 ©20XX IEEE

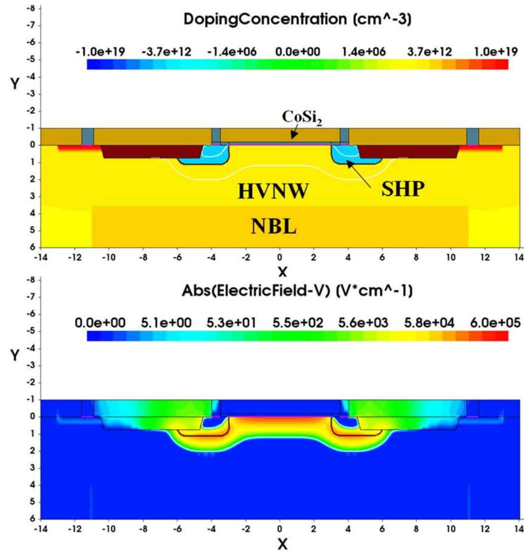

Figure 3. Simulated distributions of doping concentration (upper panel) and electric filed (lower panel). Simulation region is limited in the red dashed box in Fig 2.

The upper panel in Fig. 3 gives the distribution of doping concentration using TCAD simulation. For the lower panel in Fig. 3, we obviously observed the avalanche breakdown occurring at the Schottky junction. The maximum electric field is up to 70k V/cm, and impact ionization distribution spreads from y = 0 μm on surface to y = 1 μm. Figure 4 plots the simulated I-V curve indicating that the breakdown voltage was ~ 31.2 V.

The testing was performed with a single SPAD on chip 1 and a passive quenching circuit (PQC) on chip 2. The two dies were connected by wire bonding as shown in Fig. 5. Figure 6 schematically illustrates the experimental setup. The experiments were performed in a bark environment and the distance between SPAD chip and laser diode is 15 mm. In order to accurately measure the photocurrent, we used an optical chopper together with a lock-in amplifier to measure dark and light current. The laser (Thorlabs, ML925B45F) power was calibrated with an InGaAs photodiode (Thorlabs,

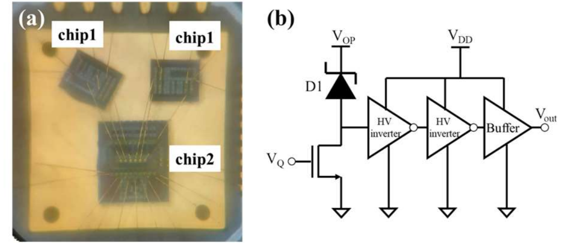

Figure 5. (a) OM photo of the t est dies of two chip 1 (dingle SPADs) and one chip 2 (Passive quenching circuit, PQC). (b) PQC schematic, where V_{OP} provides excess bias voltage (V_{EX}) and V_Q could decide the quenching resistance value.

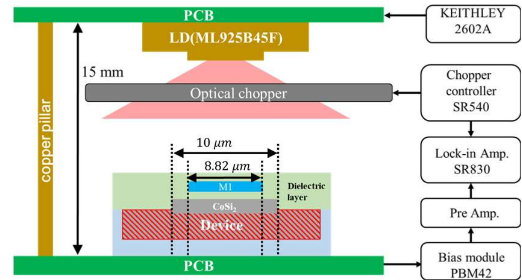

Figure 6. Schematic of the experimental setup in a dark box for the front-side illuminated photocurrent measurements.

SM05PD5A). All optical experiments were performed under front-side illumination.

III. Result and Discussion

Figure 7a shows a semi-log plot of the measured I-V curve and a typical Schottky diode is obtained. The breakdown is also observed and its breakdown voltage, which was defined with the reverse current of 1 μA, was about 31.8 V. The enlarged forward I-V in Fig. 7b was used to extract the ideal factor of ~1.05 and the Schottky barrier height of 0.646 eV which is lower than 1550-nm photon energy of 0.8 eV. The dark current of Schottky SPAD is clearly larger than that of p-n based SPAD, which may cause problems of high dark count rate (DCR) and limited dynamic range.

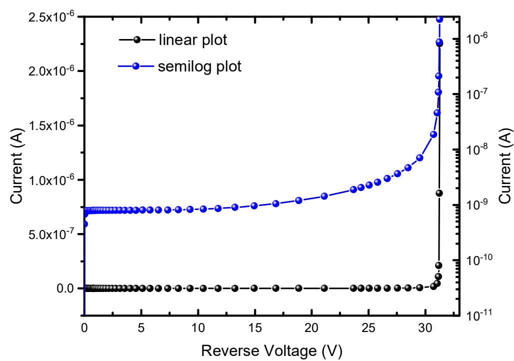

Figure 4. Simulated reverse-biased current - voltage characteristic in linear and semi-log scale.

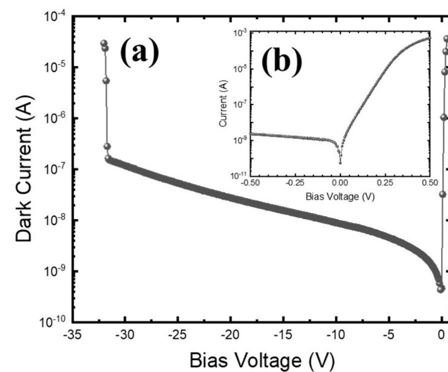

Figure 7. Measured I-V curves in (a) full range, and (b) enlarged around 0 V.

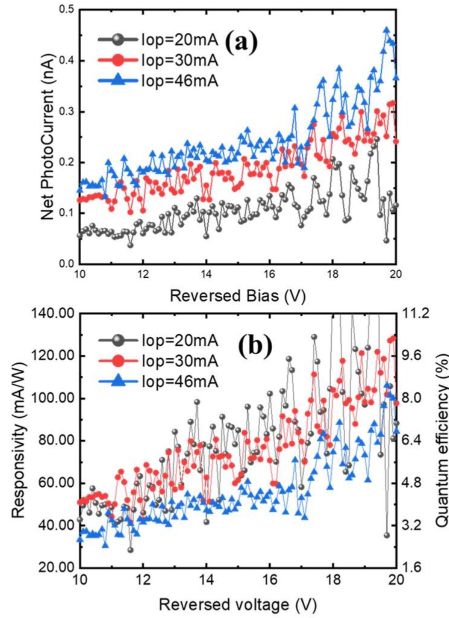

Figure 8. (a) Net Photocurrent and (b) responsivity versus Reversed bias with ML925B45F 1550nm laser diode operating on Iop = 20, 30, 46 mA.

Figure 8a shows the measured bias-dependent photocurrent under illumination from a 1550-nm continuous-wave diode laser at various intensities. Figure 8b illustrates the responsivity at 15 V of ~60 mA/W, which is pretty small probably due to the inefficient IPE effect for electron injection but showing the potential of Schottky SPAD for SWIR photon counting.

The devices suffered a few issues. For example, as shown in Fig. 9, the measured DCR were not only dependent on operating high voltage (V_{OP}) but also sensitive to quenching resistance which is controlled by quenching NMOSFET gate voltage (V_Q). This also occurred in inter-arrival time (IAT) measurement. Figure 10 shows the IAT histograms. The IAT histogram followed poissonian distribution and the after-pulsing probability was quite low.

In order to focus on the optical responsivity for Schottky-barrier based SPAD, V_{EX} and V_Q was respectively fixed at 1.0 V and 1.048 V and average deadtime was 80 ns in the following measurements. Figure 11a shows the

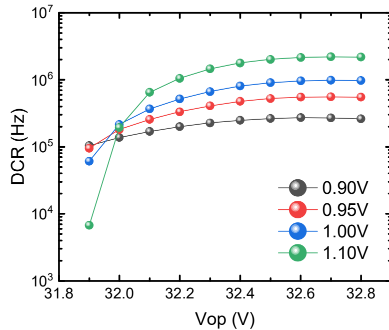

Figure 9. Dark count rate versus excessed bias for V_Q = 0.90V, 0.95V, 1.00V, and 1.10V.

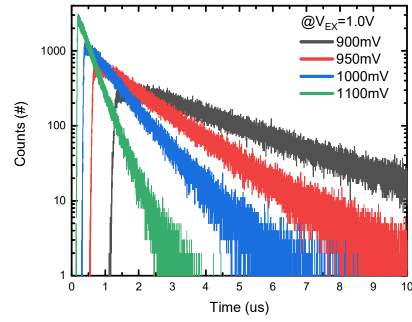

Figure 10. Histogram of inter-arrival time for V_Q = 0.90V, 0.95V, 1.00V, and 1.10V at excess bias = 1.5V.

intensity-dependent photocurrent under illumination from a 1550-nm continuous-wave diode laser measured by the lock-in method mentioned above. The result indicates early photocurrent saturation occurred at the illuminated power of 0.21 pW although the laser diode was operated in linear regime. Figure 11b shows measured intensity-dependent dark and light counts with their respective standard deviations on left y-axis and photon detection probability (PDP) on right y-axis. The Schottky-SPAD has a lower dynamic range because the light count non-linearly observed at the laser operating current of 0.8 mA. In the photocurrent and the PDP measurements, the results evidence the optical response to SWIR photons with early saturation. However, the physical mechanism of the saturation is unknown. We reckon that may be caused by the interface trap related dynamics, such as the recombination and generation at the metal-semiconductor interface. Further works are certainly needed to investigate its Geiger mode operation and quenching behavior to explain

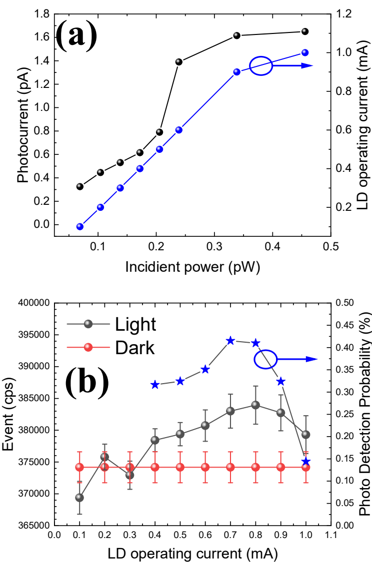

Figure 11. (a)Photocurrent and laser diode (LD) operating current versus incident power and (b) dark and light counting and photon detection probability versus LD operating current

the unusual dependence of DCR/PDP on the excess bias and the quenching resistance.

IV. CONCULSION

We demonstrate a SWIR photon counting detector with Schottky-barrier based SPAD. The devices were fabricated in a conventional CMOS process with integrated passive quenching circuits. We have successfully realized silicon-only SWIR detector. For 1550-nm photons, the Schottky SPAD obtained the responsivity of ~60 mA/W at 15 V and the PDP of ~0.35%. It unfortunately has a very low dynamic region partly because of the intrinsic high dark current of the Schottky diode. Among the bias-dependent characteristics, the quenching resistance and excess bias voltage could play a key role in the junction biasing condition as well as the measured DCR.

ACKNOWLEDGMENT: THIS WORK IS FUNDED BY THE NATIONAL SCIENCE AND TECHNOLOGY COUNCIL (NSTC) IN TAIWAN (NO. 111-2221-E-A49 -141 -MY3). THE CHIP TAPEOUT SUPPORT FROM TAIWAN SEMICONDUCTOR RESEARCH INSITITUTE (TSRI) IS HIGHLY APPRICIATED.

REFERENCES

[1] F. Villa, F. Severini, F. Madonini, and F. Zappa, “SPADs and SiPMs Arrays for Long-Range High Speed Light Detection and Ranging (LiDAR),” *Sensors*, vol. 21, pp. 3839, Apr. 2021.

[2] F. Zhao, H. Jiang, and Z. Liu, “Recent development of automotive LiDAR technology, industry and trends,” *Proc. SPIE*. Vol. 11179, pp. 1132-1139, Aug. 2019.

[3] D. C. Dumas, J. Kirdoda, R. Millar, P. Vines, and K.Kuzmenko, “High-efficiency Ge-on-Si SPADs for short wave infrared,” *Proc SPIE*, vol. 10914, pp. 389-395, Feb. 2019.

[4] F. Signorelli, F. Telesca, E. Conca, A. Della Frera, A. Ruggeri, A. Giudice, and A. Tosi, “InGaAs/InP SPAD detecting single photons at 1550 nm with up to 50% efficiency and low noise,” IEDM, pp. 20-3, Dec. 2021.

[5] T. Staffas, M. Brunzell, S. Gyger, L. Schweickert, S. Steinhaurt, and V. Zwiller, “3D scanning quantum LIDAR,” CLEO: Applications and Technology, pp. AM2K.1, May 2022.

[6] W. Diels, M. Steyaert, and F. Tavernier, “Schottky diodes in 40nnm bulk CMOS for 1310 nm high-speed optical receivers,” OFC, pp. 1-3, Mar. 2017.

[7] T. Maeda, M. Okada, M. Ueno, Y. Yamamoto, and M. Horitia, and J. Suda, Appl. Phys. Express, vol. 9, pp. 091002, Aug. 2016.